Atmos. Chem. Phys., 4, 2161–2170, 2004
www.atmos-chem-phys.org/acp/4/2161/
SRef-ID: 1680-7324/acp/2004-4-2161

Atmospheric Chemistry and Physics

A Lagrangian model with simple primary and secondary aerosol scheme 1: comparison with UK PM_{10} data

K. M. Emmerson[1], A. R. MacKenzie[2], S. M. Owen[2], M. J. Evans[3], and D. E. Shallcross[4]

[1]Environment Department, University of York, YO10 5DD, UK
[2]Dept. of Environmental Science, Lancaster University, LA1 4YQ, UK
[3]Harvard University, Cambridge, MA 02138, USA
[4]School of Chemistry, University of Bristol, BS8 1TS, UK

Received: 24 February 2004 – Published in Atmos. Chem. Phys. Discuss.: 15 June 2004
Revised: 13 September 2004 – Accepted: 5 November 2004 – Published: 9 November 2004

Abstract. A Lagrangian trajectory model used to simulate photochemistry has been extended to include a simple parameterisation of primary and secondary aerosol particles. The model uses emission inventories of primary particles for the UK from the NAEI (National Atmospheric Emissions Inventory for the UK), and for Europe from the TNO (Institute of Environmental Sciences, Energy Research and Process Innovation, the Netherlands) respectively, to transport tracers representing PM_{10}. One biogenic and two anthropogenic organic compounds were chosen as surrogates to model the formation of condensable material suitable for the production of secondary organic aerosol (SOA). The SOA is added to the primary PM_{10} and compared to measured PM_{10} at one urban and two rural UK receptor sites. The results show an average under-prediction by factors of 4.5 and 8.9 in the urban and rural cases respectively. The model is also used to simulate production of two secondary inorganic species, H_2SO_4 and HNO_3, which are assumed, as a limiting case, to be present in the particle phase. The relationships between modelled and measured total PM_{10} improved with the addition of secondary inorganic compounds, and the overall model under-prediction factors are reduced to 3.5 and 3.9 in the urban and rural cases respectively. Nevertheless, our conclusion is that current emissions and chemistry do not appear to provide sufficient information to model PM_{10} well (i.e. to within a factor of two). There is a need for further process studies to inform global climate modelling that includes climate forcing by aerosol.

Correspondence to: K. M. Emmerson
(ke7@york.ac.uk)

1 Introduction

Many previous studies of aerosol particles, and especially of secondary aerosol, have focussed on sulphates (IPCC, 2001), while little is known about the behaviour of organic compounds with regard to particulate production and their effects on climate change. Organic compounds are usually the most important component, after sulphate, of the smaller size fraction of aerosol particles in the troposphere (Heintzenberg, 1989). It is possible that organic aerosol particles are able to produce a similar (but opposite in sign) radiative effect to that produced by sulphate aerosol particles (IPCC, 2001).

Most aerosol particles are assumed to be composed of a mixture of materials, incorporating both the solid and liquid phases. Particles that are directly emitted (as a direct product of combustion, for example) are termed primary particles. Particles are also produced from reactions between gases, which yield products sufficiently involatile to partition between the gas and particle phases. Particles formed in this way are termed secondary particles.

CiTTyCAT is a Lagrangian box model that simulates the chemical processes in the atmosphere (Evans et al., 2000). It was developed to reproduce the processes affecting the production and lifetime of relatively short-lived species such as ozone. The original chemistry scheme used volatile organic compounds (VOCs) from C_2 to C_7 (e.g. toluene, C_7H_8). We have extended CiTTyCAT to include an aerosol module, incorporating primary particles together with the contribution of secondary organic aerosol (SOA) from anthropogenic and biogenic sources, and secondary inorganic aerosol (SIA) from sulphuric and nitric acids.

It has been estimated that 80% of the total SOA produced from aromatic compounds in Europe results from reactions with gas phase toluene, *p*-xylene and ethylbenzene (Derwent and Malcolm, 2000; Odum et al., 1997). Xylene and toluene

do not have reasonably well established reaction mechanisms (e.g. Calvert et al., 2002), yet have produced condensable material within a smog chamber environment (Pandis et al., 1992). Jenkin (1996) has also published an oxidation scheme for α-pinene that includes the formation of biogenic condensable material. The importance of biogenic compounds in the production of SOA is discussed in Pandis et al. (1991), Hoffmann et al. (1997), Christoffersen et al. (1998) and Hallquist et al. (1999).

2 Model treatment of particulate matter

2.1 Primary particles

The TNO provide European emissions of anthropogenic primary PM_{10} that cover the whole of Europe on a $0.5^\circ \times 1^\circ$ grid (TNO, 1997). There is a weekday-to-weekend variation in the emissions, based on 20% less mass being emitted at the weekend than during the working week (pers. comm., TNO). As yet, no seasonal cycle has been implemented. Central and Eastern Europe dominate the TNO emissions, which is due to the concentration of heavy industry in that region (ApSimon et al., 2001). A second PM_{10} inventory from the NAEI has been nested within the TNO inventory, covering the United Kingdom (including Northern Ireland) on a 1×1 km grid for 1996.

The primary PM_{10} is treated as an inert species, and no chemistry occurs. Dry deposition applies, and is based on gravitational settling via Stoke's law, assuming that all particles have a diameter of 10 μm. We choose the maximum size for all PM_{10} particles because the mass distribution is dominated by the largest particles. We show below that the model results are not very sensitive to the deposition rate and, hence to the assumed particle size. For a particle of 10 μm diameter with a deposition rate of 0.6 cm s^{-1}, this has a lifetime of approximately 2 days within a 1 km boundary layer. There is no treatment for wet deposition.

2.2 Anthropogenic and biogenic emission rates

Non-methane VOC emission rates from the EMEP 50×50 km grid for 1998 (available from http://www.emep.int) have been speciated using estimates from the Photochemical Oxidant Review Group (PORG, 1997). This method of splitting the total NMVOC emission rate has been compared to the NAEI's 50 most abundantly emitted compounds in Great Britain (the latest, year 2000 version available at http://www.naei.org.uk/) and found to contain similar species. From a total NMVOC emission rate of 94.5×10^6 kg yr^{-1}, the available species within CiTTyCAT received 50% of this total. Xylene and ethylbenzene both have the formula C_8H_{10} and a molecular weight of 106 g mol^{-1}, thus are included as a lumped xylene compound. The atmospheric chemistry of xylene and ethylbenzene are similar (Atkinson, 2000), and a single generalised reaction scheme suffices for both compounds. The lumped xylene compound and toluene are initialised with a concentration of 0 ppb.

Biogenic compounds are not included in the PORG report (1997) speciation estimate, and are treated separately. Previous modelling studies (e.g. Derwent and Malcolm, 2000) have used the Guenther et al. (1995) Global algorithm and the Simpson et al. (1999) European algorithm. The algorithms generate inventories of isoprene and monoterpene emission rates, based on land cover, land use information and meteorology. However, a recent study (Stewart et al., 2003) showed that monoterpene emission rates for Great Britain have been over-estimated by a factor of 2 by Guenther et al. (1995), and under-estimated by a factor of 2 by Simpson et al. (1999). Stewart (2001) completed a data-based study of all isoprene and monoterpene emitting vegetation in Great Britain at a resolution of 1 km^2. As these data were not available as a spatially dis-aggregated dataset at the time of writing, it is assumed for the purposes of this modelling study, that α-pinene is emitted constantly over every cm^2 of Great Britain, i.e. assuming an even distribution of vegetation. The proportion of monoterpenes emitted as α-pinene in the model is estimated to be 50%. This is a higher estimate than Griffin et al. (1999) who estimate that 35% of global monoterpene emissions are attributed to α-pinene. It should be noted that the model response to increasing emissions is linear (see Sect. 4). The α-pinene emission rate is seasonally adjusted to emit 50% more mass in summer than in winter (Stewart, 2001), as the monoterpene flux is dependent on temperature (Dement et al., 1975). The majority of monoterpene-emitting vegetation in Great Britain is not light dependent, but this is not true of species native to the European continent (Owen et al., 2002; Schuh et al., 1997). Air parcels traversing over the European continent receive twice the UK average emission rate for α-pinene, to account for higher emissions in Europe that are due to greater afforestation and higher temperatures (Simpson et al., 1999). For the purposes of the simplified scheme presented here, light dependency of monoterpene emissions is not included and α-pinene is emitted throughout the night. The European TNO grid provides the land mask for estimating the location of α-pinene emissions.

It is recognised that a large ($\sim$50%) proportion of the total PM_{10} mass could be composed of SIA. HNO_3 and H_2SO_4 are inorganic secondary species produced from the chemical reactions of NO_2 and SO_2, respectively, and both schemes are represented in CiTTyCAT (see below). Emissions of NO_2 and SO_2 are supplied from the EMEP 50×50 km grid for 1998.

2.3 Organic chemistry

The SOA chemical scheme is described in detail in a report by Jenkin (1996) and has since been redeveloped as part of the wider Master Chemical Mechanism available at http://www.chem.leeds.ac.uk/Atmospheric/

MCM/mcmproj.html (Jenkin et al., 2003 and Saunders et al., 2003). The reaction mechanisms for the lumped xylene compound and toluene are very similar, in that the parent gas-phase products react only with OH. Reactions with O_3 and NO_3 are not significant in this scheme due to the slow reaction rates. The condensable product from the toluene scheme, "TOLY", represents all C_7 nitrocresols and hydroxy nitrocresols. TOLY, whilst being subject to dry deposition, is also lost chemically through oxidation by OH and NO_3. Another model parameter, "LMXYLY", represents all C_8 nitrocresols and hydroxy nitrocresols from the lumped xylene scheme, and will produce more condensable product than TOLY due to faster reaction rates.

The biogenic compound, α-pinene, reacts with OH, NO_3 and O_3, producing pinonaldehyde in all cases as the second product. The condensable product, represented here as the "secondary biogenic component", is a carboxylic acid possibly related to pinonic acid ($C_{10}H_{16}O_3$), and has been assigned a molecular weight of $184\,g\,mol^{-1}$. The secondary biogenic component is produced through the reaction of α-pinene with O_3 in 2 steps, or in 4 steps via the reaction with OH and NO_3. The reaction with OH is the fastest however, and is the more favoured reaction pathway.

2.4 Inorganic chemistry

Nitric acid, HNO_3 is formed via the reaction of O_3 and NO_2, and reaction of OH with NO_2.

$$NO_2 + O_3 \longrightarrow NO_3 + O_2 \quad (1)$$

$$NO_3 + NO_2(+M) \leftrightarrow N_2O_5(+M) \quad (2)$$

$$N_2O_5 + H_2O \longrightarrow 2HNO_3 \quad (3)$$

$$OH + NO_2(+M) \longrightarrow HNO_3(+M) \quad (4)$$

The rate of removal of N_2O_5 to produce HNO_3 is variable, and may take a few minutes in urban areas, but can be of the order of a few hours in remote regions (PORG, 1997 and references therein). HNO_3 can produce NO_x ($NO+NO_2$) and OH through very slow photolysis reactions, but the overall reaction direction favours HNO_3 as a sink for the NO_3 species. HNO_3 is a semi-volatile inorganic compound, which is able to partition between the gas and particle phases. Once in the particle phase, HNO_3 can be removed from the atmosphere permanently through aerosol depositional processes, but it will also deposit very rapidly in the gas phase. Sulphuric acid, H_2SO_4, is involatile and always present in the particle phase. H_2SO_4 is produced through oxidation of sulphur dioxide, SO_2, which is emitted ubiquitously through both anthropogenic and natural sources.

$$SO_2 + OH(+M) \longrightarrow HSO_3(+M) \quad (5)$$

$$HSO_3 + O_2 \longrightarrow SO_3 + HO_2 \quad (6)$$

$$SO_3 + H_2O(+M) \longrightarrow H_2SO_4(+M) \quad (7)$$

There are other routes for SO_2 oxidation (Calvert et al., 1978) and N_2O_5 hydrolysis (Jacob, 2000) in the liquid phase, which are also not considered here. There are many uncertainties with regard to the uptake parameters in heterogeneous chemical modelling (e.g. DeMore et al., 1994).

2.5 Transfer of condensable material to the particle phase

For any condensable material, once saturation in the gas phase is exceeded, equilibrium with the vapour is re-established by converting a portion equal to the concentration in excess of saturation into the particle phase (Pandis et al., 1992). This process only increases the size of existing particles and does not lead to the nucleation of a new particle, as this involves surmounting a critical energy barrier. The condensation of material into the particle phase does not require any additional energy. If particles exist, and the gas phase concentration becomes less than the vapour pressure, equilibrium is reached again through evaporation from the particle surface into the gas phase. If the saturation concentration in the gas phase is greater than the total concentration available in the particle phase, then the particle will evaporate completely and leave a particulate mass of zero. This may occur if the emission rate into the gas phase is suddenly reduced, for example, if the air parcel travels from the land out over the sea. Evaporation can also occur if the temperature of the air parcel increases, thus increasing the compound vapour pressure. The saturation vapour pressure also depends on the composition of the condensed phase material, especially when a mixture is present (not treated in CiTTyCAT).

It is assumed that both anthropogenic condensable gas phase products LMXYLY and TOLY have the same vapour pressure, V_P (Torr), which is dependent on temperature (Eq. 8; Jenkin, 1996). The vapour pressure of the secondary biogenic component is treated separately (Eq. 9).

$$\log_{10}(V_P) = -3.25 - \frac{1450}{T} \quad (8)$$

$$\log_{10}(V_{Pbio}) = 15.94 - \frac{7141}{T} \quad (9)$$

These vapour pressures are towards the upper limit of what might be expected for the partitioning of the semi-volatile into an organic solid-solution. An examination of the model sensitivity to Vp = 0 is dealt with in a subsequent paper (Emmerson et al., 2004, in preparation[1]) and produced on average, 50% more SOA mass. However, with total modelled SOA mass concentrations below $1\,\mu g\,m^3$, partitioning all condensable material into the particle phase did not improve the overall modelled case significantly.

[1] Emmerson, K. M., MacKenzie, A. R., and Owen, S. M.: Development of a secondary organic aerosol module 2: Application to Europe, in preparation, 2004.

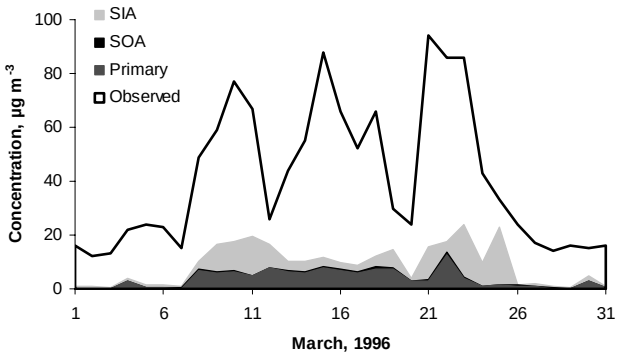

Fig. 1. Time series to show the modelled contribution of SIA, SOA and primary PM_{10} to the measured PM_{10} concentrations at Newcastle during March 1996.

Partitioning does not occur in CiTTyCAT for HNO_3 and H_2SO_4 because it is assumed that all condensable material will immediately convert into the particle phase, and no partitioning will be necessary. In real terms, H_2SO_4 is always present in the particle phase, whilst HNO_3 is semi-volatile and present in both gas and particle phases simultaneously. Usually particle phase HNO_3 is associated with the liquid phase, and is only found in dry aerosol if ammonia is present (Hewitt, 2001 and references therein). However, there is no ammonia present in the model and it is not known what fraction of HNO_3 is present in the gas phase at any particular time.

The total mass concentration of particles produced from these new schemes will be added to the concentration of modelled primary PM_{10}. A dry deposition rate of $0.2\,cm\,s^{-1}$ is assigned for the SOA and SIA, equivalent to smaller particles with diameters of $0.1\,\mu m$ (or $PM_{0.1}$) and a density of $1.6\,g\,cm^{-3}$. This is equivalent to an atmospheric residence time of just under 6 days in a 1 km boundary layer.

3 Model receptor sites

The model follows 3-dimensional, 4-day back trajectories. These are supplied by the British Atmospheric Data Centre (BADC) trajectory service, which is available on-line at http://www.badc.rl.ac.uk. 4 trajectories per day were used ending at midnight, 6 am, 12 noon and 6 pm. As the measurements were provided as 24 h averages the modelled data was averaged to provide 1 data point per day. All trajectories are calculated using 3-D advection to end at 950 mbars (∼530 m), which usually avoids the problem of air parcel trajectories intersecting the surface and terminating early. As the model assumes that emissions are mixed homogeneously through the height of the boundary layer (which can reach heights of 2 km), calculating the transport at a height of 530 m is reasonable. Boundary layer heights are taken from an assimilation of data from the GEOS 1 meteorological satellite, which is archived on a 2.5° longitude by 2° latitude grid (Schubert et al., 1993). The data within this grid is assumed to be sufficient to account for all time periods, and therefore does not restrict the use of CiTTyCAT to a particular time for which satellite data was available.

The urban receptor site chosen for this study is Newcastle, in the north east of the UK (1.60° W, 55.0° N) for the months of March and July 1996. These months were chosen to complement the study of particulate sulphates by Malcolm et al. (2000). The Newcastle site is a "background urban" site, 30 m from the nearest road. Two rural sites, Narberth in west Wales (4.75° W, 51.75° N) and Rochester in east Kent (0.55° E, 51.40° N), are also analysed for March 1998. Average PM_{10} at Rochester was half of that at Newcastle during this month. This was a month with little rainfall and is more appropriate for the processes studied here (recall that there is no treatment for wet deposition). Since the PM_{10} signal is the sum of primary and secondary, carbonaceous and inorganic fractions, it is convenient to have a benchmark aerosol composition in mind, in order to assess qualitatively how the various parts of the model are performing. Urban and rural measurements in Europe (e.g. Kuhlbusch et al., 1999; Zappoli et al., 1999; Harrison et al., 1997) suggest that the total organic fraction (primary and secondary carbon) is a maximum of 40% of total PM_{10}, and the secondary inorganic fraction a further 50%, the majority of which is composed of sulphate. Other secondary inorganic species are not accounted for in this study, particularly ammonium and chloride, and could provide the remaining 10%. There were no clear patterns between urban and rural sites to suggest that primary/secondary ratio is much larger at urban locations. Emmerson (2002) provides a detailed explanation of how these estimates are made. Below, we will refer to these broad composition fractions as the expected mass percentages. This does not mean that we believe the composition of the aerosol is constant in time and space, but rather that the expected composition provides a rough guide to which parts of the model are performing well. These expected mass percentages allow us to calculate model under-prediction factors, which are the factors by which the model under-predicts not the whole observed mass, but just that part of the whole mass that the model might be expected to under-predict. The total modelled time series mass concentrations were then compared to the total measured PM_{10} mass concentrations at each site, taken from the NETCEN automated network (available at http://www.airquality.co.uk).

3.1 Urban Newcastle site, March 1996

Figure 1 shows the addition of the modelled SOA and SIA contributions to primary PM_{10}. Three relationships are obtained from the modelled and measured data and shown in Table 1. The first shows the linear correlation between concentrations of primary PM_{10} with the observed PM_{10} concentration. The second relationship is the linear correlation

Table 1. Coefficients of determination, average mass percentages and model under-prediction factors in the modelled species for each of the receptor sites studied here. Under-prediction factor calculations are based on assumed aerosol compositions of 30% primary PM_{10}, 40% primary PM_{10}+SOA, and 90% primary PM_{10}+SOA+SIA. SOA is secondary organic aerosol; SIA is secondary inorganic aerosol.

Location	Date	Primary			Primary+SOA			Primary+SOA+SIA		
		R^2	Average mass %	Under prediction factor	R^2	Average mass %	Under prediction factor	R^2	Average mass%	Under prediction factor
Newcastle	03 1996	0.49	9	3.3	0.51	10	4.0	0.57	22	4.5
Newcastle	07 1996	0.61	6	5.0	0.63	8	5.0	0.66	40	2.5
Narberth	03 1998	0.13	2	15.0	0.14	3	13.3	0.08	18	5.6
Rochester	03 1998	0.30	8	3.8	0.30	9	4.4	0.41	47	2.1

Factor values >1 represent an under-prediction. Factor values=1 represent a perfect match. Factor values <1 represent an over-prediction.

between concentrations of modelled primary PM_{10} and SOA only with the measured PM_{10} concentrations. The third relationship is between the modelled primary PM_{10}, SOA, and total SIA concentrations and the measured PM_{10} concentrations. The coefficients of determination (R^2) and the percentage of the total measured mass that is modelled on average, increase as each component of the model is added-in. However the under-prediction factors also increase.

The modelled peak of 19 $\mu g\,m^{-3}$ in the primary PM_{10} around the 21–22 March, occurs on the same date as the peak in the observed data. Correlating all the modelled and measured data gives an R^2 value of 0.49. The modelled SOA has provided no more than 0.3 $\mu g\,m^{-3}$ (on average) to the average primary PM_{10} concentration of 3.6 $\mu g\,m^{-3}$. The secondary biogenic component contributes most of the mass (98%) to the total SOA modelled, because there are very few occurrences of the anthropogenic gas phase condensable species LMXYLY and TOLY exceeding the saturation vapour pressure. Between 10 and 12 March the modelled anthropogenic secondary particles reach a maximum of 0.04 $\mu g\,m^{-3}$ in total, and there is a peak of 0.2 $\mu g\,m^{-3}$ on 23 March. This peak in the modelled anthropogenic condensable species occurs 1 day after the 22 March peak in modelled primary PM_{10}. The maximum in the modelled secondary biogenic component of 0.8 $\mu g\,m^{-3}$ occurs on 17 and 22 March, although the whole model time series for this compound exhibits strong diurnal cycles.

The combined modelled primary PM_{10} and SOA concentration of 3.9 $\mu g\,m^{-3}$ represents one quarter of the expected mass percentage (40%) from the primary and secondary organics, which is therefore under-predicted by a factor of 4. The addition of the modelled SOA to the primary PM_{10} does not significantly improve the correlation of the modelled time series compared with measurements of PM_{10} (R^2=0.51). Addition of the particle phase H_2SO_4 only to modelled PM_{10} resulted in a better correlation of modelled data to measurements (R^2=0.61). However, addition of particulate HNO_3 to the total modelled PM_{10} decreased the R^2 to 0.57. This implies that the treatment of HNO_3 as involatile is too simplistic. However all R^2 relationships are significant at the 95% confidence interval. Equal concentrations of modelled HNO_3 and H_2SO_4 are present at Newcastle during March (assuming all HNO_3 is particulate matter), with an average of 4 $\mu g\,m^{-3}$ and 5 $\mu g\,m^{-3}$ for the whole of the month, respectively. The combined modelled SIA represents 12% of the total measured PM_{10} mass, which is less than the expected 50%. The total modelled primary PM_{10}, SOA and SIA for the month of March is 22% of the observed total. Thus if the maximum mass of PM_{10} expected from all the modelled constituents is 90%, then the model has under-predicted by a factor of 4.5.

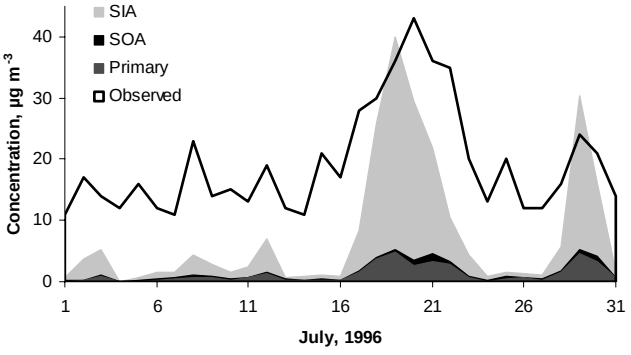

Fig. 2. Time series to show the modelled contribution of SIA, SOA and primary PM_{10} to the measured PM_{10} concentrations at Newcastle during July 1996.

3.2 Urban Newcastle, July 1996

Figure 2 shows the modelled time series of SIA, SOA and primary PM_{10} to total measured PM_{10} concentrations for the July 1996 model runs for Newcastle. Statistics for the case study are given in Table 1. CiTTyCAT results reproduce the shape of the observed values better (R^2=0.61) than for March, especially between 17–23 July. The maximum measured PM_{10} (43 $\mu g\,m^{-3}$) occurs on 19–20 July.

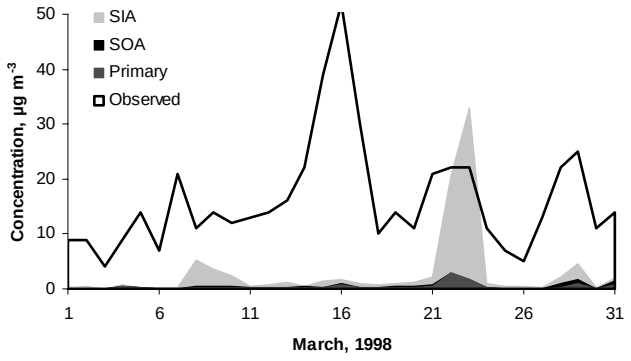

Fig. 3. Time series to show the modelled contribution of SIA, SOA and primary PM_{10} to the measured PM_{10} concentrations at Narberth during March 1998.

Secondary organic and inorganic components make a much larger contribution to the modelled PM_{10} in this summertime case. This is not as a result of seasonal fluctuations in emissions, which were applied to α-pinene for summer model runs. Instead, the concentrations of anthropogenic species in summer result from different trajectories, and hence different emission sources from those in March. Concentrations of α-pinene generated by the model for July runs are also double those modelled in March due to natural seasonal variation. A peak in the secondary biogenic component of $1.5\,\mu g\,m^{-3}$, occurs on 21 July at midnight. The mass percentage of the total modelled SOA species due to the biogenic compound alone is 95%. However, modelled primary PM_{10} concentrations for July are about a third of the modelled March concentrations. Higher concentrations of the anthropogenic compounds in July are due to localised emissions in the north east of the UK, as the trajectories spend much of their lifetime over the sea, where there are no emissions. This also suggests that there was insufficient time for a pulse of anthropogenic emissions during the final part of the trajectories to react; there are no emissions of either anthropogenic species for 3.5 days at the start of the 15 July trajectory. The total average modelled SOA concentration during July is $0.3\,\mu g\,m^{-3}$ and when added to the average modelled concentrations of primary PM_{10} of $1.2\,\mu g\,m^{-3}$ gives a total of $1.5\,\mu g\,m^{-3}$. This combined result under-predicts the estimated mass percentage from the modelled primary PM_{10} plus the SOA by a factor of 5. The addition of the modelled SOA increases the R^2 correlation to 0.63, significant at the 95% confidence level.

In the R^2 correlations for July (Table 1), the R^2 relationship is improved further with the addition of the HNO_3, unlike the March model runs. Using only H_2SO_4 together with the modelled primary PM_{10} and SOA does not improve the R^2 relationship on the 0.63 obtained with the modelled primary PM_{10} and SOA only. However, if it is assumed that all HNO_3 is in the particle phase, the correlation is improved marginally to 0.66. The improved correlation maybe fortuitous, as the temperature dependence of HNO_3 condensation is neglected. The average concentrations of HNO_3 and H_2SO_4 for the whole of July at Newcastle are $0.8\,\mu g\,m^{-3}$ and $1.5\,\mu g\,m^{-3}$, respectively. These concentrations are 4 times less than the concentrations for both particulate inorganic species modelled for the month of March at Newcastle. The peak concentration in the modelled time series occurs on 19 July, with $40\,\mu g\,m^{-3}$in total, with $25\,\mu g\,m^{-3}$ composed of HNO_3 and $10\,\mu g\,m^{-3}$ from H_2SO_4. The combined SIA contributes 32% to the total measured PM_{10} for the whole of the month, which is less than the expected 50% mass percentages for SIA. If the modelled primary PM_{10} and SOA concentrations are added to the modelled SIA concentration, the total modelled mass percentage for July at Newcastle is increased to 40%. This represents an under-prediction by a factor of 2.3 on the measured PM_{10}, which is probably due to the low concentrations of modelled primary PM_{10}.

3.3 Rural Narberth, March 1998

Figure 3 shows the time series in the combined secondary inorganic, organic and primary modelled PM_{10} at the first of the UK rural receptor sites, Narberth in west Wales. The total SOA modelled does not generally provide significant additional mass to the modelled primary PM_{10}. As with all previous SOA modelling studies in this work, the secondary biogenic component forms the greatest fraction of total modelled SOA, which is nearly 99% of the total SOA mass. However, the modelled SOA concentration contributed an extra 60% to the total modelled PM_{10} on 29 March at Narberth, increasing the modelled PM_{10} from $1\,\mu g\,m^{-3}$ to $1.6\,\mu g\,m^{-3}$. This is the only date in the Narberth study where the addition of the modelled SOA mass concentrations makes a significant difference to the shape of the total modelled time series.

Air mass trajectories on 29 March travel from France and Spain, whilst trajectories for the rest of the month travel straight across the clean Atlantic Ocean. The SOA scheme produces more particulate mass from trajectories that have traversed a greater distance across the continent. This is because there are increased emissions early on in the trajectory which have time to react before reaching the receptor site. The modelled SOA for 10 March also shows an increase over the original modelled PM_{10}, which signifies a land-based influence. The 10 March trajectory passed over the Birmingham area and picked up anthropogenic gas phase emissions, but this increase is not mirrored by the modelled primary PM_{10} as the inventories are different. PMXYLY and PMTOLY are only present on two of the 31 days in March (9 and 23 March), in the $0.01\,\mu g\,m^{-3}$ range. These anthropogenic particle species therefore produce a factor of 10 to 100 times less mass than the biogenic species, though in most cases the anthropogenic species rarely exceed their vapour pressures and so remain in the gas phase. Plotting the observed PM_{10} from NETCEN against the total modelled primary particles

plus the SOA yields an R^2 of 0.14 for Narberth. The percentage of total modelled mass of primary PM_{10} and SOA is 3% of the total measured PM_{10}, which represents an under-prediction on the expected 40% mass fraction by a factor of 13.3. Previously, the primary modelled fraction was under-predicted by a factor of 15 (shown in Table 1), so this is an improvement.

The average concentrations of HNO_3 and H_2SO_4 for the whole of March are 2.1 $\mu g\,m^{-3}$ and 0.3 $\mu g\,m^{-3}$ respectively, with a peak of 33 $\mu g\,m^{-3}$ on 23 March mainly due to HNO_3. Both the previous SIA studies at Newcastle showed a greater proportion of H_2SO_4 in the modelled results. The combined SIA modelled for Narberth forms 15% of the total measured PM_{10}, which is one third of the expected 50% mass percentages for SIA. It is likely that emissions of the gas phase precursor species are not present in the air parcel, as most of the trajectory length is out over the sea. When the modelled primary PM_{10} and SOA mass percentage is added to the modelled SIA contribution, there is still a total model under-prediction by a factor of 5.6. The R^2 correlation coefficient is reduced to 0.08 for both of the relationships shown alongside Fig. 3, from the previous modelled R^2 value of 0.14. However, none of these relationships are significant at 95%, and could have occurred by chance. Narberth is the only study where the R^2 value decreased after adding the contribution of the modelled SIA.

3.4 Rural Rochester, March 1998

The time series in the contribution of modelled SIA, SOA and primary PM_{10} combined is shown alongside the total measured PM_{10} concentration in Fig. 4 for the second UK rural site, Rochester in east Kent. There are two modelled peaks of primary PM_{10} on 16 March (4.6 $\mu g\,m^{-3}$, which is 9% of the measured PM_{10} peak of 54 $\mu g\,m^{-3}$) and 24th, though there is only peak in the measured PM_{10} on 16 March. The monthly average concentration of primary PM_{10} at Rochester represents 8% of the observed average concentration. Until 23 March the modelled SOA is around 0.05 $\mu g\,m^{-3}$, and therefore contributes little mass on top of the modelled primary PM_{10}. The trajectories for the latter period of March traverse more of the European continent and therefore produce slightly more SOA, around 0.2 $\mu g\,m^{-3}$, which is a factor of 10 greater than the particulate mass produced from the non-continental trajectories. The peak day for modelled SOA concentrations is 24 March, which yields 0.6 $\mu g\,m^{-3}$ entirely composed of the secondary biogenic component. The model calculates anthropogenic species PMXYLY and PMTOLY to be in the particle phase at Rochester on only 2 days (25 and 29 March, at concentrations of 0.05 $\mu g\,m^{-3}$. These dates at Rochester do not correspond with the same dates in March at Narberth when the anthropogenic species were modelled in the particle phase.

The R^2 of the correlations between the modelled primary and modelled primary plus SOA against measured PM_{10} at Rochester are both 0.30. The total modelled mass of PM_{10} for the Rochester case is only 9% of the total measured PM_{10}, and the expected mass is under-predicted by a factor of 4.4.

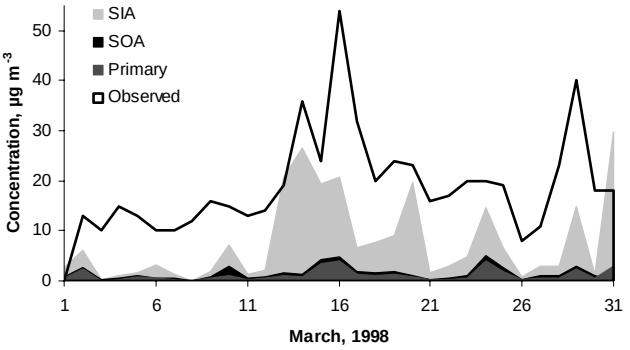

Fig. 4. Time series to show the modelled contribution of SIA, SOA and primary PM_{10} to the measured PM_{10} concentrations at Rochester during March 1998.

Both SIA correlations (i.e. H_2SO_4 only and H_2SO_4 plus HNO_3) are an improvement on the previous R^2 value of 0.30 for Rochester. The coefficients of determination are 0.36 with the addition of H_2SO_4 only, and 0.41 for the further addition of HNO_3. All R^2 values for Rochester border on significance at the 95% test level. The peaks and troughs in the modelled species shown in Fig. 4 do not reflect the smoothness of the measured data and explains why the correlation is poor. However, the modelled time series is very good for the last half of the month, with sharp peaks on 20, 24 and 29 March with 20 $\mu g\,m^{-3}$, 15 $\mu g\,m^{-3}$ and 22 $\mu g\,m^{-3}$ respectively. The average concentrations of HNO_3 and H_2SO_4 modelled for the whole month at Rochester are 6.6 $\mu g\,m^{-3}$ and 0.6 $\mu g\,m^{-3}$, respectively, again showing a dominance of HNO_3. This was also the case at Narberth, but H_2SO_4 was the more dominant SIA species for both months at Newcastle. At Rochester, the average model concentration of HNO_3 is 7 times greater than the H_2SO_4 concentration. The combined modelled inorganic species forms 38% of the total measured PM_{10}, which represents a slight under-prediction of the expected SIA mass percentage by the model. Addition of the modelled mass percentage of PM_{10} and SOA for March gives a total mass of 47% for the modelled species. This still represents an under-prediction by a factor of 1.9 on the measured PM_{10} concentrations, again assumed to be predominantly due to the under-predicted primary PM_{10}.

4 Sensitivity tests

Two sensitivity tests have been conducted which vary the model initial conditions, emission and deposition rates for the inert primary PM_{10}. In CiTTyCAT, the steady state concentration depends linearly on the emission rate E, and on the

Table 2. Results from 22 March trajectory with varying initial conditions. All concentrations in units of $\mu g\,m^{-3}$.

	Initial PM_{10}	Resultant PM_{10}
Default	0	19
European Background	16	27.3
European Background × 2	40	40
High Initial Values	120	89

reciprocal of the deposition velocity, $1/V_D$.

$$\frac{d\chi_i}{dt} = \frac{E_i}{h} - \frac{V_{Di}\chi_i}{h} \quad (10)$$

The very simple treatment of PM_{10} in CiTTyCAT will introduce some errors in the model results. The most important simplifications are (i) no wet deposition and (ii) instantaneous mixing through the height of the boundary layer. Error (i) could affect the ability of the model to capture variability in the observed time series, but not the consistent under-prediction of the observed aerosol mass. We concentrate on error (ii) here, since it is related to this first-order under-prediction error. The sensitivity to mixing height may be significant, but is not such a problem for low spatial resolution in emission inventories, and for gradual changes in emissions between adjacent emission squares, but may be considered for areas of rapidly changing emission values.

4.1 Varying initial conditions

As many of the trajectories begin over Central and Eastern Europe, it may have been more realistic to set the initial particle concentration at a European background value, rather than $0\,\mu g\,m^{-3}$. These regions are known to dominate particle emissions (ApSimon et al., 2001), and air parcels originating here are unlikely to be entirely clean. Table 2 shows the results when the trajectory for the peak concentrations on 22 March at Newcastle is re-run with varying initial concentrations. The impact is not linear, due to the self-limiting effect of the first-order deposition scheme. The first row gives the default value and the modelled outcome of $19.4\,\mu g\,m^{-3}$. The second row uses the estimated European annual average from ApSimon et al. (2001) who also used the TNO inventory. They thought that their original estimates might be under-predicted by a factor of two, and row 3 in the table reflects this. The final row shows that very high initial conditions must be used to approach the measured value of $94\,\mu g\,m^{-3}$ with the primary PM_{10} alone, yet this neglects the fact that most PM_{10} is composed of SIA.

4.2 Varying emission and deposition rates

To study the effects of varying emissions and deposition, a trajectory ending on 19 July at Newcastle, the peak in the modelled concentrations for that month, is run five times. Figure 5 shows the progression of the trajectory from day 198 as it travels towards Newcastle on day 201 (19 July). Note that approximately half of the final particulate mass is injected in half an hour (6 model time steps) as the air trajectory crosses the UK, illustrating the variability in the emission inventory. Response A shows the default model run. Responses B and C use the default emissions, but divide the deposition rates by 2 and by 5, respectively. Responses D and E use the default deposition rates, but multiply the emission rates by 2 and by 5, respectively. The choices for using the factors 2 and 5 were to test whether a reasonable under or over-prediction would help the modelling case, or whether a 400% increase in emissions was required to reach the observed concentrations. It can be seen that forcing the emissions (D and E) has more effect on the concentration of PM_{10}, than forcing the deposition rate (B and C). The end point at Newcastle on day 201 shows the original PM_{10} concentration to be 6 $\mu g\,m^{-3}$. Doubling the emissions (D), gives a PM_{10} concentration of $12\,\mu g\,m^{-3}$, and multiplying the emission rate by a factor of 5 (E) gives $30\,\mu g\,m^{-3}$. The response from CiTTyCAT is linear in the emissions for this case. The measured concentrations in Fig. 2 show that at Newcastle there was $43\,\mu g\,m^{-3}$ of PM_{10} on 19 July. If approximately 30% of the PM_{10} mass is expected to be primary in an urban area (recall that the Newcastle receptor site is not immediately beside a road), then the target for primary particles is reduced to $13\,\mu g\,m^{-3}$. This can be achieved by multiplying the primary particulate emission rates by 2. We may regard this as a rough estimate of the under-prediction of the emissions inventory, or over-prediction of the boundary layer height.

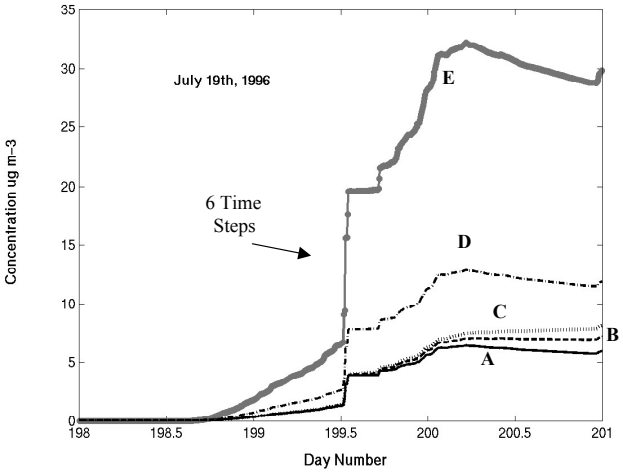

Fig. 5. Sensitivity study for trajectory ending at Newcastle on 19 July 1996 (see Fig. 2). (A) is the original response. (B) the deposition rate is halved, (C) the deposition rate is divided by 5, (D) the emission rates were doubled and (E) the emission rates multiplied by 5.

5 Conclusions

Our Lagrangian model of primary, organic secondary and inorganic secondary aerosol mass correlates at the 95% significance level with PM_{10} data measured data background urban site, but does less well compared to data at two rural sites. Although the correlations are significant, there are consistent and substantial under-predictions of average total mass concentrations and of the expected mass percentages of different combinations of aerosol components. The model can be brought closer to the observations by including a background initial concentration for PM_{10}, and/or increasing the emissions of primary particles by a factor of approximately 2.

Secondary organic aerosol mass in the model output is always a fraction of the total aerosol mass, but its inclusion does generally improve the model-data correlations. The single biogenic species produces significantly more (in excess of 80%) of the condensed particle mass in CiTTyCAT in all cases, than either of the two anthropogenic species. This reflects the reactivity of biogenic compounds and the model suggests that they could be the main contributors to SOA production. However, there was no spatial variation in the biogenic emissions, and whilst the high molecular weight compounds are more reactive (such as α-pinene), it is the C_5-C_{10} anthropogenic compounds (predominantly the aromatics) which contribute most to SOA mass concentrations in urban areas (Isodorov, 1990). It is likely that many other important C_5-C_{10} organic compounds are not accounted for in CiTTyCAT, such as other aromatics, aldehydes, alkenes and ketones. Such VOCs may also be under-estimated in the emission inventories, as measurement techniques have previously misinterpreted their importance (Lewis et al., 2000). The modelling studies undertaken with the new SOA module show minor improvements in correlation with measurements at the UK receptor sites, with the urban case showing the best improvement in the correlation coefficients between the modelled and measured PM_{10} concentrations. The modelled SOA in the UK urban case produces a factor of 2 more mass than the rural case, which highlights the emission differences incurred when the trajectories travel over the land. The correlations between primary modelled PM_{10} and the measured PM_{10} were poor, and addition of the modelled SOA did not improve the strengths or the significance of these relationships. Table 1 shows the percentages of the measured data for modelled primary PM_{10}, both with and without the modelled SOA and SIA. These calculations are based on an expected 30% by mass for modelling the primary PM_{10} only, an expected 40% for the primary PM_{10} plus the SOA, and an expected 90% for modelled primary PM_{10}, SOA and SIA combined. Generally, the model under-prediction decreases as further species are added. This suggests that if all PM_{10} species were accounted for explicitly in the model, the relationships between modelled and measured PM_{10} will continue to improve. A perfect correlation (i.e. R^2=1) between such explicit species modelling and measurements is unlikely, as not all compounds that contribute to PM_{10} will be accounted for and to some extent parameterisations must be used. In addition, the transport and mixing of the air can never be modelled accurately. In spite of the inherent limitations of these process modelling studies, it seems clear that more process studies are necessary to support global climate modelling that includes aerosol forcing, to improve confidence that the emissions inventories and model structures are sufficiently accurate to yield useful estimates of aerosol loading. A companion paper studying European receptor sites (EMO, 2004) aims to further this understanding.

Acknowledgements. The authors would like to thank H. Stewart and D. Lowe of the atmospheric interactions group at Lancaster University for providing expertise with the biogenic emissions and computer programming, respectively. KME would like to acknowledge her studentship from the UK Universities Global Atmospheric Modelling Programme (UGAMP). CiTTyCAT is a product of UGAMP's Atmospheric Chemistry Support Unit, at the University Chemical Laboratory, Cambridge, UK.

Edited by: T. Hoffmann

References

ApSimon, H. M., Gonzalez del Campo, M. T., and Adams, H. S.: Modelling long-range transport of primary particulate material over Europe, Atmos. Environ., 35, 343–352, 2001.

Atkinson, R.: Atmospheric chemistry of VOCs and NO_x, Atmos. Environ., 34, 2063–2101, 2000.

Calvert, J. G., Atkinson, R., Becker, K. H., Seinfeld, J. H., Wallington, T. J., and Yarwood, G.: The mechanism of atmospheric oxidation of aromatic hydrocarbons. Oxford University Press, New York, ISBN 0-19-524628-X, 2002.

Calvert, J. G., Su, F., Bottenheim, J. W., and Strausz, O. P.: Mechanism of the homogeneous oxidation of sulphur dioxide in the troposphere, Atmos. Environ., 12, 197–226, 1997.

Christoffersen, T. S., Hjorth, J., Horie, O., Jensen, N. R., Kotzias, D., Molander, L. L., Neeb, P., Ruppert, L., Winterhalter, R., Virkkula, A., Wirtz, K., and Larsen, B. R.: Cis-pinic acid, a possible precursor for organic aerosol formation from ozonolysis of α-pinene, Atmos. Environ., 32, 1657–1661, 1998.

Dement, W. A., Tyson, B. J., and Mooney, H. A.: Mechanism of monoterpene volatilisation in Salvia mellifera, Phytochemistry, 14, 2555–2557, 1975.

DeMore, W. B., Sander, S. P., Golden, D. M., Hampson, R. F., Kurylo, M. J., Howard, C. J., Ravishankara, A. R., Kolb, C. E., and Molina, M. J.: Chemical kinetics and data for use in stratospheric modelling, Eval 11, Jet Propulsion Laboratory, Pasadena, California, 1994.

Derwent, R. G. and Malcolm, A. L.: Photochemical generation of secondary particles in the United Kingdom, Phil. Trans. R. Soc. Lond, 358, 2643–2657, 2000.

Emmerson, K. M.: Modelling the production of organic atmospheric aerosol, PhD thesis, Lancaster University, 2002.

Evans, M. J., Shallcross, D. E., Law, K. S., Wild, J. O. F., Simmonds, P. G., Spain, T. G., Berrisford, P., Methven, J. V., Lewis,

A. C., McQuaid, J. B., Pilling, M. J., Bandy, B. J., Penkett, S. A., and Pyle, J. A: Validation of a Lagrangian box model using field measurements from EASE (Eastern Atlantic Summer Experiment) 1996, Atmos. Environ., 34, 3843–3863, 2000.

Griffin, R. J., Cocker, D. R. III., Seinfeld, J. H., and Dabdub, D. R.: Estimate of global organic aerosol from oxidation of biogenic hydrocarbons, Geophys. Res. Lett, 26, 2721–2724, 1999.

Guenther, A., Hewitt, C. N., Erickson, D., Fall, R., Geron, C., Graedel, T., Harley, P., Klinger, L., Lerdau, M., McKay, W. A., Pierce, T., Scholes, B., Steinbrecher, R., Tallamraju, R., Taylor, J., and Zimmerman, P.: A global model of natural volatile organic compound emissions, J. Geophys. Res., 100, 8873–8892, 1995.

Harrison, R. M., Deacon, A. R., Jones, M. R., and Appleby, R. S.: Sources and processes affecting concentrations of PM_{10} and $PM_{2.5}$ particulate matter in Birmingham (UK), Atmos. Environ., 31, 4103–4117, 1997.

Hallquist, M., Wängberg, I., Ljungström, E., Barnes, I., and Becker, K. H.: Aerosol and product yields from NO_3 radical initiated oxidation of selected monoterpenes, Environ. Sci. Technol., 33, 553–559, 1999.

Heintzenberg, J.: Fine particles in the global troposphere: A review, Tellus B, 41, 149–160, 1989.

Hoffmann, T., Odum, J. R., Bowman, F., Collins, D., Klockow, D., Flagan, R. C., and Seinfeld, J. H.: Formation of organic atmospheric aerosols from the oxidation of biogenic hydrocarbons, J. Atmos. Chem., 26, 189–222, 1997.

Intergovernmental Panel on Climate Change (IPCC): Climate change 2001: The scientific basis, edited by: Houghton, J. T., Ding, Y., and Griggs, D. J., et al., Cambridge University Press, 2001.

Isodorov, V. A.: organic chemistry of the earth's atmosphere, Springer-Verlag, Berlin, 1990.

Jacob, D. J.: Heterogeneous chemistry and tropospheric ozone, Atmos. Environ., 34, 2131–2159, 2000.

Jenkin, M. E.: Chemical mechanisms forming condensable material, AEA Technology Report, AEA/RAMP/20010010/002, 1996.

Jenkin, M. E., Saunders, S. M., Wagner, V., and Pilling, M. J.: Protocol for the development of the Master Chemical Mechanism, MCM v3 (Part B): Tropospheric degradation of aromatic volatile organic compounds, Atmos. Chem. Phys, 3, 181–193, 2003,
SRef-ID: 1680-7324/acp/2003-3-181.

Kuhlbusch, T. A. J., John, A. C., Fissan, H., Schmidt, K.-G., Schmidt, F., Pfeffer, H.-U., and Gladtke, D.: PM_{10} and $PM_{2.5}$ mass concentration, chemical composition, and size distribution measurements at three different sites in the Ruhr area, Germany, J. Aerosol Sci., 30, S45–S46, 1999.

Lewis, A. C., Carslaw, N., Marriott, P. J., Kinghorn, R. M., Morrison, P., Lee, A. M., Bartle, K. D., and Pilling, M. J.: A larger pool of ozone-forming carbon compounds in urban atmospheres, Nature, 405, 778–781, 2000.

Malcolm, A. L., Derwent, R. G., and Maryon, R. H.: Modelling the long range transport of secondary PM_{10} to the UK, Atmos. Environ., 34, 881–894, 2000.

Odum, J. R., Hoffmann, T., Bowman, F., Collins, D., Flagan, R. C., and Seinfeld, J. H.: Gas/particle partitioning and secondary organic aerosol yields, Environ. Sci. Technol., 30, 2580–2585, 1996.

Owen, S. M., Harley, P. Guenther, A., and Hewitt, C. N.: Light dependency of VOC emissions from selected Mediterranean plant species, Atmos. Environ., 36, 3147–3159, 2002.

Pandis, S. N., Harley, R. A., Cass, G. R., and Seinfeld, J. H.: Secondary organic aerosol formation and transport, Atmos. Environ., 26A, 2269–2282, 1992.

Pandis, S. N., Paulson, S. E., Seinfeld, J. H., and Flagan, R. C.: Aerosol formation in the photo-oxidation of isoprene and β-pinene, Atmos. Environ., 25A, 997–1005, 1991.

Photochemical Oxidants Review Group (PORG): Ozone in the United Kingdom, Fourth report, 1997.

Saunders, S. M., Jenkin, M. E., Derwent, R. G., and Pilling, M. J.: Protocol for the development of the Master Chemical Mechanism, MCM v3 (Part A): Tropospheric degradation of non-aromatic volatile organic compounds, Atmos. Chem. Phys., 3, 161–180, 2003,
SRef-ID: 1680-7324/acp/2003-3-161.

Schubert, S. D., Rood, R. B., and Pfaendtner, J.: An assimilated data set for earth science applications, Bulletin of the American meteorological Society, 74, No. 12, 1993.

Schuh, G., Heiden, A. C., Hoffmann, T., Kahl, J., Rockel, P., Rudolph, J., and Wildt, J.: Emissions of volatile organic compounds from sunflower and beech: Dependence on temperature and light intensity, J. Atmos. Chem., 27, (3), 291–318, 1997.

Simpson, D., Winiwarter, W., Borjesson, G., Cinderby, S., Ferreiro, A., Guenther, A., Hewitt, C. N., Jansen, R., Khalil, M. A. K., Owen, S., Pierce, T. E., Puxbaum, H., Shearer, M., Skiba, U., Steinbrecher, R., Tarrason, L., and Oquist, M. G.: Inventorying emissions from nature in Europe, J. Geophys. Res., 104, 8113–8152, 1999.

Stewart, H. E.: The development of a biogenic isoprene and monoterpene emission inventory for Great Britain, PhD thesis, Lancaster University, 2001.

Stewart, H. E., Hewitt, C. N., Bunce, R. G. H., Steinbrecher, R., Smiatek, G., and Schoenemeyer, T.: A highly spatially and temporally resolved inventory for biogenic isoprene and monoterpene emissions – model description and application to Great Britain, J. Geophys. Res, 108 (D20), 4644, doi:10.1029/2002JD002694, 2003.

TNO.: Particulate matter emissions (PM_{10}–$PM_{2.5}$–$PM_{0.1}$) in Europe in 1990 and 1993, Report TNO-MEP-R96/472, Netherlands, February 1997, 1997.

Zappoli, S., Andracchio, A., Fuzzi, S., Facchini, M. C., Gelenoser, A., Kiss, G., Krivacsy, Z., Molnar, A., Meszaros, E., Hansson, H-C., Rosman, K., and Zebuhr, Y.: Inorganic, organic and macromolecular components of fine aerosol in different areas of Europe in relation to their water solubility, Atmos. Environ., 33, 2733–2743, 1999.